Determining global mean-first-passage time of random walks on Vicsek fractals using eigenvalues of Laplacian matrices

Zhongzhi Zhang,[1,2,*] Bin Wu,[1,2] Hongjuan Zhang,[2,3] Shuigeng Zhou,[1,2,†] Jihong Guan,[4,‡] and Zhigang Wang[5]

[1]*School of Computer Science, Fudan University, Shanghai 200433, China*
[2]*Shanghai Key Lab of Intelligent Information Processing, Fudan University, Shanghai 200433, China*
[3]*Department of Mathematics, College of Science, Shanghai University, Shanghai 200444, China*
[4]*Department of Computer Science and Technology, Tongji University, 4800 Cao'an Road, Shanghai 201804, China*
[5]*Mahle Technologies Holding (China) Co., Ltd., Shanghai 201400, China*

The family of Vicsek fractals is one of the most important and frequently studied regular fractal classes, and it is of considerable interest to understand the dynamical processes on this treelike fractal family. In this paper, we investigate discrete random walks on the Vicsek fractals, with the aim to obtain the exact solutions to the global mean-first-passage time (GMFPT), defined as the average of first-passage time (FPT) between two nodes over the whole family of fractals. Based on the known connections between FPTs, effective resistance, and the eigenvalues of graph Laplacian, we determine implicitly the GMFPT of the Vicsek fractals, which is corroborated by numerical results. The obtained closed-form solution shows that the GMFPT approximately grows as a power-law function with system size (number of all nodes), with the exponent lies between 1 and 2. We then provide both the upper bound and lower bound for GMFPT of general trees, and show that the leading behavior of the upper bound is the square of system size and the dominating scaling of the lower bound varies linearly with system size. We also show that the upper bound can be achieved in linear chains and the lower bound can be reached in star graphs. This study provides a comprehensive understanding of random walks on the Vicsek fractals and general treelike networks.

I. INTRODUCTION

Fractals are an important concept characterizing the features of real systems, because they can model a broad range of objects in nature and society [1]. Over the past few decades, fractals have attracted considerable interest from the physics community [2,3]. Among numerous fractal classes, the so-called regular fractals are an integral family of fractals. Examples include the Sierpinski gasket [4], the Koch snowflake [5], the Vicsek fractals [6], and so on. These structures have received much attention [1–3] and continue to be an active object of research [7]. One of the main reasons for studying regular fractals is that one can obtain explicit closed-form solutions on a finite structure. Another justification is that various problems intractable on Euclidean lattices become solvable on regular fractals [8]. On the other hand, the exact solutions on regular fractals can provide useful insight different from that given by the approximate solutions for random fractals.

A central issue, still debated, is to understand how the underlying geometrical and structural features influence various dynamics defined on complex systems, which has been considered to be an important problem in many interdisciplinary fields, e.g. network science [9–11]. Amongst a plethora of fundamental dynamical processes, random walks are crucial to a lot of branches of sciences and engineering and have appealed much interest [2,12–14]. A basic quantity relevant to random walks is first-passage time (FPT) [15], which is the expected time to hit a target node for the first time for a walker staring from a source node. It is a quantitative indicator to characterize the transport efficiency and carries much information of random walks since many other quantities can be expressed in terms of it. Thus, a growing number of studies have been concentrated on this interesting quantity [16–23].

In view of the significance of regular fractals and random-walk dynamics, many authors have devoted their endeavors to study random walk on regular fractals [24], such as the Sierpinski gasket [25,26], the *T*-fractal [27–29], the Vicsek fractals [30,31], as well as the hierarchical lattice fractals [32,33]. The results of these investigations unveiled many unusual and exotic phenomena of random walks on regular fractals. But in the aspect of FPT, these studies only addressed the mean of FPTs between part of the node pairs, e.g., between a given node and all other nodes [25,26,29,33], while the scaling for the FPT averaged over all pairs of nodes, often called global mean-first-passage time (GMFPT), in the regular fractals is still not well understood [20], in spite that GMFPT provides comprehensive information of random walks on fractals and other media.

In this paper, we study analytically the discrete random walks on a class of treelike fractals—Vicsek fractals, which are typical candidates for exact mathematical fractals and have received extensive interest [34–38]. We determine exactly the GMFPT between two nodes over the whole fractal family, which is verified by numerical results. The closed-form formula for the GMFPT is achieved iteratively by using the advantage of the specific construction of the Vicsek fractals. The obtained explicit expression indicates that for large

*zhangzz@fudan.edu.cn
†sgzhou@fudan.edu.cn
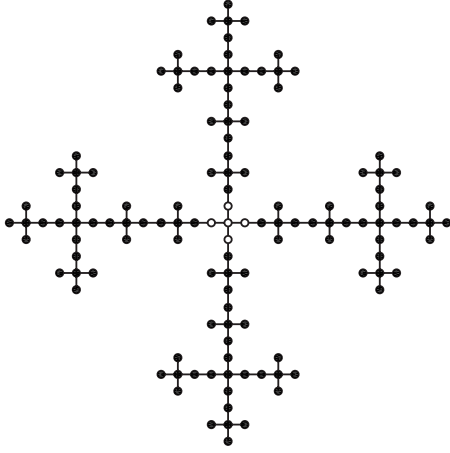‡jhguan@tongji.edu.cn

FIG. 1. Illustration of the first several iterative processes of a particular Vicsek fractal $V_{4,3}$. The open circles denote the starting structure $V_{4,1}$.

systems the GMFPT increases algebraically with the size of the systems. In the second part of this work, we provide the rigorous upper and lower bounds for GMFPT as a function of system size for general treelike media. We show that of all trees linear chains have the largest value of GMFPT and the star graphs have the smallest GMFPT.

II. BRIEF INTRODUCTION TO THE VICSEK FRACTALS

The so-called Vicsek fractals are constructed in an iterative way [6,35]. Let $V_{f,g}$ ($f \geq 2$, $g \geq 1$) denote the Vicsek fractals after g iterations (generations). The construction starts from ($g=1$) a starlike cluster consisting of $f+1$ nodes arranged in a crosswise pattern, where f peripheral nodes are connected to a central node. This corresponds to $V_{f,1}$. For $g \geq 2$, $V_{f,g}$ is obtained from $V_{f,g-1}$. To obtain $V_{f,2}$, we generate f replicas of $V_{f,1}$ and arrange them around the periphery of the original $V_{f,1}$, then we connect the central structure by f additional links to the corner copy structure. These replication and connection steps are repeated infinitely, with the needed Vicsek fractals obtained in the limit $g \rightarrow \infty$, whose fractal dimension is $\ln(f+1)/\ln 3$. In Fig. 1, we show schematically the structure of $V_{4,3}$. According to the construction algorithm, at each step the number of nodes in the systems increases by a factor of $f+1$, thus, we can easily know that the total number of nodes (i.e., network order or system size) of $V_{f,g}$ is $N_g = (f+1)^g$. Since the whole family of Vicsek fractals has a treelike structure, the total number of links in $V_{f,g}$ is $E_g = N_g - 1 = (f+1)^g - 1$.

III. GMFPT IN THE VICSEK FRACTALS

After introducing the Vicsek fractals $V_{f,g}$, we will continue to study numerically and analytically random walks performed on them, which is the primary topic of this present paper. The random-walk model we study is a simple one. Assuming the time to be discrete, at each time step, the walker (or particle) jumps uniformly from its current location to one of its neighbors. The highly desirable quantity
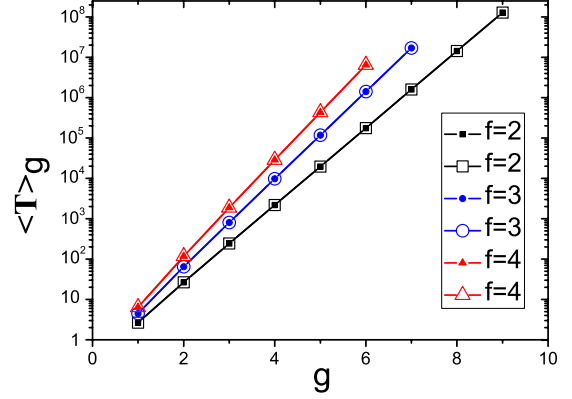
related to random walks is the GMFPT starting from a source point to a given target point, averaged over all node pairs of source and target points.

The GMFPT can be obtained numerically but exactly via the pseudoinverse [39,40] of the Laplacian matrix, $\mathbf{L}_g$, of $V_{f,g}$. The entries L_{ij}^g of $\mathbf{L}_g$ are defined as follows: the off-diagonal element $L_{ij}^g = -1$ if the pair of nodes i and j are linked to each other, otherwise $L_{ij}^g = 0$; while the diagonal entry $L_{ii}^{(g)} = d_i$ (degree of node i). The pseudoinverse (denoted by $\mathbf{L}_g^\dagger$) of $\mathbf{L}_g$ is a variant of its inverse matrix and is defined to be

$$\mathbf{L}_g^\dagger = \left(\mathbf{L}_g - \frac{\mathbf{e}_g \mathbf{e}_g^\top}{N_g} \right)^{-1} + \frac{\mathbf{e}_g \mathbf{e}_g^\top}{N_g}, \tag{1}$$

where $\mathbf{e}_g$ is the N_g-dimensional "one" vector, i.e., $\mathbf{e}_g = (1,1,\ldots,1)^\top$.

The FPT between any pair of nodes in $V_{f,g}$ can be expressed in terms of the elements, $L_{ij}^{\dagger,g}$, of $\mathbf{L}_g^\dagger$. Let $T_{ij}(g)$ stand for the FPT for random walks in $V_{f,g}$, starting from node i to node j. Then [41]

$$T_{ij}(g) = \sum_{n=1}^{N_g} (L_{in}^{\dagger,g} - L_{ij}^{\dagger,g} - L_{jn}^{\dagger,g} + L_{jj}^{\dagger,g}) L_{nn}^g, \tag{2}$$

where L_{nn}^g is the nth diagonal entry of $\mathbf{L}_g$. Thus, the sum, $T_{\text{sum}}(g)$, for FPTs between all node pairs in $V_{f,g}$ reads as

$$T_{\text{sum}}(g) = \sum_{i \neq j} \sum_{j=1}^{N_g} T_{ij}(g), \tag{3}$$

and the GMFPT, $\langle T \rangle_g$, is

$$\langle T \rangle_g = \frac{T_{\text{sum}}(g)}{N_g(N_g - 1)} = \frac{1}{N_g(N_g - 1)} \sum_{i \neq j} \sum_{j=1}^{N_g} T_{ij}(g). \tag{4}$$

Using Eqs. (2) and (4), we can compute directly the GMFPT $\langle T \rangle_g$ of the Vicsek fractals (see Fig. 2). From Fig. 2, we can see that $\langle T \rangle_g$ approximately grows exponentially in g. In

FIG. 2. (Color online) Global mean-first-passage time $\langle T \rangle_g$ as a function of the iteration g on a semilogarithmic scale for different parameter f. The filled symbols are the numerical results obtained by direct calculation from Eqs. (2) and (4), while the empty symbols correspond to the exact values from Eq. (18), both of which are consistent with each other.

other words, $\langle T \rangle_g$ is a power-law function of network order N_g obeying the scaling as $\langle T \rangle_g \sim (N_g)^\theta$ since $N_g = (f+1)^g$. It should be mentioned that although the expression of Eq. (4) seems compact, it requires computing the inversion of a matrix of order $N_g \times N_g$ [see Eq. (1)], which make heavy demands on time and computational resources for large networks. Thus, one can calculate directly from Eq. (4) the GMFPT only for the first iterations. On the other hand, by using the method of pseudoinverse matrix it is difficult and even impossible to obtain the leading behavior of the exponent θ characterizing the random walks. It is thus of significant practical importance to seek for a computationally cheaper method for computing the GMFPT. Fortunately, the particular construction of the Vicsek fractals and the connection [42,43] between effective resistance and the FPTs for random walks allow us to calculate analytically the GMFPT and the exponent θ to obtain rigorous solutions.

Below we will show how to avoid the computational complexity of inverting a matrix. To this end, we view $V_{f,g}$ as resistor networks [44] by considering each edge to be a unit resistor. Let $R_{ij}(g)$ be the effective resistance between two nodes i and j in the electrical networks obtained from $V_{f,g}$. Then, according to the relation between FPTs and effective resistance [42,43], we have

$$T_{ij}(g) + T_{ji}(g) = 2E_g R_{ij}(g). \tag{5}$$

Therefore, Eq. (3) can be rewritten as

$$T_{\text{sum}}(g) = E_g \sum_{i \neq j} \sum_{j=1}^{N_g} R_{ij}(g). \tag{6}$$

Using the previously obtained results [45,46], the sum term on the right-hand side of Eq. (6) denoted by $R_{\text{sum}}(g)$ can be recast as

$$R_{\text{sum}}(g) = \sum_{i \neq j} \sum_{j=1}^{N_g} R_{ij}(g) = 2N_g \sum_{i=2}^{N_g} \frac{1}{\lambda_i^{(g)}}, \tag{7}$$

where $\lambda_i^{(g)}$ ($i=2,\ldots,N_g$) are all the nonzero eigenvalues of Laplacian matrix, $\mathbf{L}_g$, of the Vicsek fractals $V_{f,g}$. Then, we have

$$\langle T \rangle_g = 2 \sum_{i=2}^{N_g} \frac{1}{\lambda_i^{(g)}}. \tag{8}$$

Having $\langle T \rangle_g$ in terms of the sum of the reciprocal of all nonzero Laplacian eigenvalues, the next step is to determine this sum.

The determination of all eigenvalues of $\mathbf{L}_g$ can be resolved by using the real-space decimation method [47,48]. Assuming that one has the eigenvalues $\lambda_i^{(g)}$ ($\lambda_i^{(g)} \neq 0$) at generation g, then the eigenvalues $\lambda_i^{(g+1)}$ of the next generation $g+1$ can be obtained through the relation [49–51]

$$\lambda_i^{(g+1)}(\lambda_i^{(g+1)} - 3)(\lambda_i^{(g+1)} - f - 1) = \lambda_i^{(g)}. \tag{9}$$

By solving Eq. (9), each eigenvalue $\lambda_i^{(g)}$ ($\lambda_i^{(g)} \neq 0$) at generation g gives rise to three new and different ones at generation $g+1$, denoted by $\lambda_{i,1}^{(g+1)}$, $\lambda_{i,2}^{(g+1)}$, and $\lambda_{i,3}^{(g+1)}$, respectively. Moreover, the newly generated eigenvalues keep the degeneracy

of their ancestors. Considering that all the nonzero eigenvalues of $V_{f,1}$ are $\lambda_i^{(1)} = 1$ ($i=2,3,\ldots,f$) and $\lambda_{f+1}^{(1)} = f+1$, one can obtain all nonzero eigenvalues $\lambda_i^{(g)}$ of $\mathbf{L}_g$ by iteratively solving Eq. (9) $g-1$ times.

It should be stressed that although we can provide $\lambda_i^{(g)}$ in a recursive way, it is difficult to write $\lambda_i^{(g)}$ in an explicit formula. However, in what follows we will show that the recursive solution to $\lambda_i^{(g)}$ allows to obtain a closed-form expression for the sum of the reciprocal of all nonzero eigenvalues of $\mathbf{L}_g$, denoted by Λ_g. By definition

$$\Lambda_g = \sum_{i=2}^{N_g} \frac{1}{\lambda_i^{(g)}}. \tag{10}$$

A main goal of the following text is to explicitly determining this sum.

Let Ω_g express the set of all the N_g eigenvalues of $\mathbf{L}_g$, i.e., $\Omega_g = \{\lambda_1^{(g)}, \lambda_2^{(g)}, \ldots, \lambda_{N_g}^{(g)}\}$, where the distinctness of the elements has been ignored. Notice that all these eigenvalues are either nondegenerate or degenerate [51]. The set of the former is denoted by $\Omega_g^{(1)}$, while the set of the latter is denoted by $\Omega_g^{(2)}$. That is to say, $\Omega_g = \Omega_g^{(1)} \cup \Omega_g^{(2)}$. $\Omega_g^{(1)}$ includes 0, $f+1$ and other eigenvalues generated by the "seed" $\lambda_{f+1}^{(1)} = f+1$; and $\Omega_g^{(2)}$ includes 1 and other eigenvalues derived from 1. Furthermore, the degeneracy of the degenerate eigenvalues rests with the generation at which they appeared at the first time. At a given generation j, the degeneracy of eigenvalues 1 is $\Delta_j = (f-2)(f+1)^{j-1} + 1$, a degeneracy that their descendants keep. In what follows, for convenience we use $\Omega_g^{(1)}$ to represent the nondegenerate eigenvalues of $\mathbf{L}_g$ other than 0.

We now return to derive Λ_g, which can be evidently recast as

$$\Lambda_g = \sum_{\lambda_i^{(g)} \in \Omega_g^{(1)}} \frac{1}{\lambda_i^{(g)}} + \sum_{\lambda_i^{(g)} \in \Omega_g^{(2)}} \frac{1}{\lambda_i^{(g)}}. \tag{11}$$

We denote the two sums on the right-hand side of Eq. (11) by $\Lambda_g^{(1)}$, and $\Lambda_g^{(2)}$, respectively. Below we will calculate the two quantities $\Lambda_g^{(1)}$ and $\Lambda_g^{(2)}$.

We first calculate $\Lambda_g^{(1)}$. At the initial generation 1, there is only one nondegenerate eigenvalue $f+1$, which produces three different nondegenerate eigenvalues at generation 2. We call these three eigenvalues the first-generation descendants of $f+1$, which give rise to 3^2 second-generation descendants of $f+1$ at the third generation. Thus, at ith generation, 3^{i-1} $(i-1)$th-generation descendants of $f+1$ are produced. Since all eigenvalues (degenerate or nondegenerate) which appeared at one generation will still appear in all subsequent generations [49–51], we have $\Omega_{g-1}^{(1)} \subset \Omega_g^{(1)}$. Hence, as noted above, $\Omega_g^{(1)}$ consists of $f+1$ and all its offspring produced after generation 1.

Let $\Gamma_i^{(1)}$ be the sum of the reciprocal of all the $(i-1)$th-generation descendants of $f+1$. Then, $\Lambda_g^{(1)}$ can be rewritten in terms of $\Gamma_i^{(1)}$ as

$$\Lambda_g^{(1)} = \sum_{i=0}^{g-1} \Gamma_i^{(1)}, \tag{12}$$

where $\Gamma_0^{(1)} = \Lambda_1^{(1)} = 1/(f+1)$.

Note that for each nonzero eigenvalue (degenerate or nondegenerate) $\lambda_i^{(g)} \in \Omega_g$, Eq. (9) can be rewritten in an alternative way as

$$(\lambda_i^{(g+1)})^3 - (f+4)(\lambda_i^{(g+1)})^2 + 3(f+1)\lambda_i^{(g+1)} - \lambda_i^{(g)} = 0. \tag{13}$$

According to the Vieta's formulas, the three roots (i.e., $\lambda_{i,1}^{(g+1)}$, $\lambda_{i,2}^{(g+1)}$, and $\lambda_{i,3}^{(g+1)}$) of Eq. (13) satisfy the following two relations: $\lambda_{i,1}^{(g+1)} \cdot \lambda_{i,2}^{(g+1)} \cdot \lambda_{i,3}^{(g+1)} = \lambda_i^{(g)}$ and

$$\lambda_{i,1}^{(g+1)} \cdot \lambda_{i,2}^{(g+1)} + \lambda_{i,1}^{(g+1)} \cdot \lambda_{i,3}^{(g+1)} + \lambda_{i,2}^{(g+1)} \cdot \lambda_{i,3}^{(g+1)} = 3(f+1).$$

Thus,

$$1/\lambda_{i,1}^{(g+1)} + 1/\lambda_{i,2}^{(g+1)} + 1/\lambda_{i,3}^{(g+1)} = 3(f+1)/\lambda_i^{(g)}.$$

Based on the results obtained above, we have

$$\Gamma_g^{(1)} = \sum_{\lambda_i^{(g)} \in \Omega_g^{(1)} \backslash \Omega_{g-1}^{(1)}} \frac{3(f+1)}{\lambda_i^{(g)}} = 3(f+1)\Gamma_{g-1}^{(1)}, \tag{14}$$

which together with the initial condition $\Gamma_0^{(1)} = 1/(f+1)$ leads to $\Gamma_g^{(1)} = 3^g(f+1)^{g-1}$. Inserting this result into Eq. (12), we get

$$\Lambda_g^{(1)} = \sum_{i=0}^{g-1} [3^i(f+1)^{i-1}] = \frac{1}{f+1}\frac{3^g(f+1)^g - 1}{3f+2}. \tag{15}$$

After obtaining $\Lambda_g^{(1)}$, all that is left to find an expression for Λ_g is to evaluate $\Lambda_g^{(2)}$. For each eigenvalue 1, applying an approach similar to that used above, we can compute the sum of the reciprocal of its $(i-1)$th-generation descendants, which we represent by $\Upsilon_i^{(2)}$. After some simple algebra, we obtain $\Upsilon_i^{(2)} = 3^i(f+1)^i$ ($0 \le i \le g-1$), where $\Upsilon_0^{(2)} = 1$ express the reciprocal of the "seed" eigenvalue 1 itself. It has been shown that [49–51] in the Vicsek fractals $V_{f,g}$, the degeneracy of eigenvalues 1 is $\Delta_g = (f-2)(f+1)^{g-1} + 1$, and the degeneracy of each of its ith-generation ($0 \le i \le g-1$) offspring is $\Delta_{g-i} = (f-2)(f+1)^{g-1-i} + 1$. Then, the quantity $\Lambda_g^{(2)}$ is evaluated as follows:

$$\Lambda_g^{(2)} = \sum_{i=0}^{g-1} (\Delta_{g-i} \cdot \Upsilon_i^{(2)})$$

$$= \frac{(f-2)(f+1)^{g-1}(3^g-1)}{2} + \frac{3^g(f+1)^g - 1}{3f+2}, \tag{16}$$

Plugging Eqs. (15) and (16) into Eq. (11) yields

$$\Lambda_g = \frac{(f-2)(f+1)^{g-1}(3^g-1)}{2} + \frac{f+2}{f+1}\frac{3^g(f+1)^g - 1}{3f+2}. \tag{17}$$

Using the relation $\langle T \rangle_g = 2\Lambda_g$, we have

$$\langle T \rangle_g = (f-2)(f+1)^{g-1}(3^g-1) + \frac{2(f+2)}{f+1}\frac{3^g(f+1)^g - 1}{3f+2}. \tag{18}$$

We have confirmed this closed-form expression for $\langle T \rangle_g$ against direct computation from Eqs. (2) and (4). For all range of g and different f, they completely agree with each other, which shows that the analytical formula provided by Eq. (18) is right. Figure 2 shows the comparison between the numerical and predicted results, with the latter plotted by the full expression for the sum in Eq. (18).

We can also support the validity of Eq. (18) by using another method. In fact, the correctness of Eq. (18) depends on all the nonzero Laplacian eigenvalues, the exactness for derivation of which can be established according to the relation between the Laplacian eigenvalues and the number of spanning trees of a graph. It has been established that the number of spanning tress on a connected graph G with order N, $N_{st}(G)$, is related to all its nonzero Laplacian eigenvalues λ_i (assuming $\lambda_1 = 0$ and $\lambda_i \ne 0$ for $i = 2, \dots, N$), obeying the relation $N_{st}(G) = \frac{1}{N}\Pi_{i=2}^{N}\lambda_i$ [52]. Since the Vicsek fractals $V_{f,g}$ are trees, the product of all nonzero Laplacian eigenvalues for $V_{f,g}$, denoted by Θ_g, should equal N_g, which can be corroborated by the following argument. By definition, $\Theta_g = \Theta_g^{(1)} \cdot \Theta_g^{(2)}$, where $\Theta_g^{(i)}$ ($i = 1, 2$) is the product of Laplacian eigenvalues in $\Omega_g^{(i)}$. Applying the Vieta's formulae, we can easily obtained the product of the ith-order ($0 \le i \le g-1$) offspring of the "seed" eigenvalue $f+1$ is $f+1$, which is independent of i. Then $\Theta_g^{(1)} = (f+1)^g$. Similarly, we have $\Theta_g^{(2)} = 1$. Hence, $\Theta_g = (f+1)^g = N_g$, which proves the correctness of the computation on the Laplacian eigenvalues for $V_{f,g}$.

We proceed to show how to represent GMFPT, $\langle T \rangle_g$, as a function of the network order N_g, with the aim to obtain the relation between these two quantities. Recalling $N_g = (f+1)^g$, we have $3^g = (N_g)^{\ln 3/\ln(f+1)}$ that enables one to write $\langle T \rangle_g$ in the following form:

$$\langle T \rangle_g = \frac{f-2}{f+1}N_g[(N_g)^{\ln 3/\ln(f+1)} - 1]$$

$$+ \frac{2(f+2)}{(f+1)(3f+2)}[(N_g)^{1+\ln 3/\ln(f+1)} - 1]. \tag{19}$$

Equation (19) unveils the explicit dependence relation of GMFPT on network order N_g and parameter f. For large systems, i.e., $N_g \to \infty$, we have following expression for the dominating term of $\langle T \rangle_g$,

$$\langle T \rangle_g \sim \frac{f(3f-2)}{(f+1)(3f+2)}(N_g)^{1+\ln 3/\ln(f+1)}$$

$$= \frac{f(3f-2)}{(f+1)(3f+2)}(N_g)^{\theta}$$

$$= \frac{f(3f-2)}{(f+1)(3f+2)}(N_g)^{2/\tilde{d}} \tag{20}$$

where $\tilde{d} = 2\ln(f+1)/\ln(3f+3)$ is the spectral dimension of the Viskek fractals [51]. Thus, in the large limit of g, the GMFPT grows approximately as a power-law function of
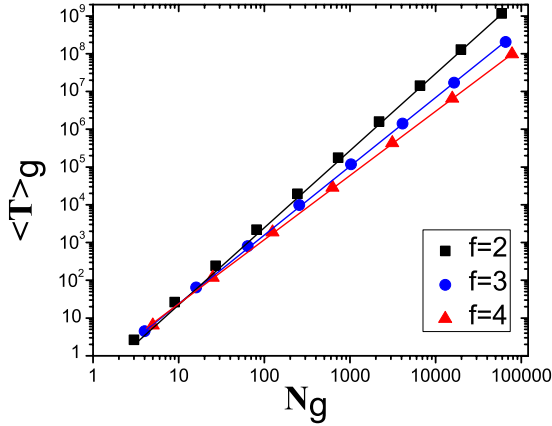
FIG. 3. (Color online) Global mean-first-passage time $\langle T \rangle_g$ versus the network order N_g on a log-log scale. The filled symbols described the analytic results shown in Eq. (18). The solid lines represent the corresponding leading scaling given by Eq. (20).

network order N_g with the exponent $\theta = 1 + \ln 3 / \ln(f+1)$ being a decreasing function of f. It is easy to see that the exponent θ is larger than 1 but not greater than 2. Particularly, when $f=2$, θ reduces to 2, which is the highest one reported thus far. In fact, 2 is largest exponent for GMFPT of random walks defined on treelike media, the rigorous proof of which will be given in the next section. In addition, it should be mentioned that the obtained superlinear dependence of GMFPT on the network order is in contrast with the other scalings previously observed for other media, e.g., linear scaling for the Apollonian networks [53] and the pseudofractal scale-free web [54], a logarithmic correction to the linear dependence for small-world trees [21,23]. Figure 3 shows how the GMFPT scales with the network order for various parameter f.

IV. BOUNDS FOR GMFPT IN TREES

In Sec. III, we have shown that the GMFPT in the Vicsek fractals scales as a power-law function of network order. Previous studies exhibited that GMFPT in other trees may depend on network order N following different scalings. For example, in the deterministic uniform recursive trees, their GMFPT varies with network order N as $N \ln N$ [55]; in the T-fractal, the GMFPT grows as $N^{1+\ln 2/\ln 3}$ [56]. These show that in different trees, the GMFPT obeys different dependence relation on network order. Then, some natural questions arise: what are the upper and lower bounds for GMFPT in general trees? In which trees are these bounds reached?

As a matter of fact, the above questions are equivalent to find the upper and lower bounds for the total effective resistance, R_{sum}, as defined similarly by Eq. (7). One can prove with ease using various methods [57–61] that for trees with order N, the upper and lower bounds for R_{sum} are

$$R_{\text{sum}}^{\text{Upp}} = \frac{N(N-1)(N+1)}{3} \quad (21)$$

and

$$R_{\text{sum}}^{\text{Low}} = 2(N-1)^2, \quad (22)$$

respectively.

The upper bound can be only reached for the tree that is exactly a linear chain (a path), which has two nodes with degree 1 at both ends of the chain and $N-2$ nodes with degree 2 in the middle [60]. Actually, this linear chain is one of the particular Viscek fractals corresponding to $f=2$. The result provided by Eq. (21) is compatible with that of the Vicsek fractals corresponding to $f=2$. As for the lower bound, it can be only achieved when the tree is a star graph [58,59,61], consisting of one central node and $N-1$ leaf nodes. All these leaf nodes are linked to the central node, and there is no edge between the leaf nodes.

From Eqs. (21) and (22), we can easily obtain that the upper and lower bounds for GMFPT are

$$\langle T \rangle^{\text{Upp}} = \frac{(N-1)(N+1)}{3} \quad (23)$$

and

$$\langle T \rangle^{\text{Low}} = \frac{2(N-1)^2}{N}, \quad (24)$$

respectively. Thus, the GMFPT $\langle T \rangle$ for general trees satisfies the relation $\langle T \rangle^{\text{Upp}} \leq \langle T \rangle \leq \langle T \rangle^{\text{Low}}$. For large trees (i.e., $N \to \infty$), the leading scalings for $\langle T \rangle^{\text{Upp}}$ and $\langle T \rangle^{\text{Low}}$ change separately with network order N as $\langle T \rangle^{\text{Upp}} \sim N$ and $\langle T \rangle^{\text{Low}} \sim N^2$, implying that the scaling for the GMFPT in any tree must lie between linear scaling and square of network order. It is very obvious that the upper bound is much larger than the lower bound, the reasons for which lie with the underlying structures of the corresponding graphs: the linear chain is homogeneous, while the star graph is heterogeneous.

In the star graphs, the central node has a very large degree, and thus plays a crucial role in keeping the whole graph together. When the random-walk process is performed in the star graphs, the walker has a tendency to migrate toward the central node, through which it jumps to the target nodes. Therefore, the efficiency of random walks is very high in the star graphs, the linear scaling of the GMFPT with N is the best we can see [61]. Notice that the same scaling has been previously observed for complete graphs [54]. In fact, the star graphs can be obtained from the complete graph with the same order by whittling down complete graphs, i.e., by the judiciously removing edges from complete graphs leaving only one node with $N-1$ connections, in order that the walker in the star graphs can find the destination nodes as easily as in the complete graphs.

On the contrary, in the linear chains all nodes are homogenous. When the walker starting from the source point to find the target node far away from the staring point, it must traverse all nodes between the starting point and the destination node. This makes the traverse time much longer than in the star graphs.

Finally, we should stress that although the star graphs are extreme of heterogeneous media, they are very instructive to understand the dynamics of random walks on other heterogeneous graphs, especially scale-free networks [62], which

are ubiquitous in real natural and social systems [63,64]. Previous studies have shown that random walks in scale-free networks are very efficient [33,54,65–69], the roots of which is actually can be heuristically explained as above. The large-degree nodes in scale-free networks play a similar role as that of the central node in the star graphs, making the GMFPT very small.

V. CONCLUSIONS

We have studied the discrete random walks on the family of Vicsek fractals, which includes the linear chains as a particular case. Using the connection between the FPTs and the Laplacian eigenvalues for general graphs, we have computed the GMFPT averaged over all pairs of nodes in the fractals and obtained explicit solutions to the GMFPT. The obtained closed-form formula shows that in the limit of infinite network order N, the GMFPT $\langle T \rangle$ grows approximately as a power-law function of N: $\langle T \rangle \sim N^{1+\ln 3/\ln(\bar{f}+1)}$. We have also provided rigorous bounds on the network order dependence of the GMFPT in general treelike networks. We showed that the upper and lower bounds can be achieved in linear chains and star graphs, respectively. Our study sheds useful insights into the random-walk process occurring on treelike media.

[1] B. Mandlebrot, *The Fractal Geometry of Nature* (Freeman, San Francisco, 1982).

[2] S. Havlin and D. ben-Avraham, Adv. Phys. **36**, 695 (1987).

[3] D. ben-Avraham and S. Havlin, *Diffusion and Reactions in Fractals and Disordered Media* (Cambridge University Press, Cambridge, 2000).

[4] W. Sierpinski, Compt. Rend. **160**, 302 (1915).

[5] H. von Koch, Acta Math. **30**, 145 (1906).

[6] T. Vicsek, J. Phys. A **16**, L647 (1983).

[7] K. J. Falconer, *Fractal Geometry: Mathematical Foundations and Applications* (Wiley, Chichester, 2003).

[8] W. A. Schwalm, M. K. Schwalm, and M. Giona, Phys. Rev. E **55**, 6741 (1997).

[9] M. E. J. Newman, SIAM Rev. **45**, 167 (2003).

[10] S. Boccaletti, V. Latora, Y. Moreno, M. Chavez, and D.-U. Hwanga, Phys. Rep. **424**, 175 (2006).

[11] S. N. Dorogovtsev, A. V. Goltsev, and J. F. F. Mendes, Rev. Mod. Phys. **80**, 1275 (2008).

[12] R. Metzler and J. Klafter, Phys. Rep. **339**, 1 (2000).

[13] R. Metzler and J. Klafter, J. Phys. A **37**, R161 (2004).

[14] R. Burioni and D. Cassi, J. Phys. A **38**, R45 (2005).

[15] S. Redner, *A Guide to First-Passage Processes* (Cambridge University Press, Cambridge, 2001).

[16] E. W. Montroll, J. Math. Phys. **10**, 753 (1969).

[17] J. D. Noh and H. Rieger, Phys. Rev. Lett. **92**, 118701 (2004).

[18] S. Condamin, O. Bénichou, and M. Moreau, Phys. Rev. Lett. **95**, 260601 (2005).

[19] V. Sood, S. Redner, and D. ben-Avraham, J. Phys. A **38**, 109 (2005).

[20] S. Condamin, O. Bénichou, V. Tejedor, R. Voituriez, and J. Klafter, Nature (London) **450**, 77 (2007).

[21] A. Baronchelli, M. Catanzaro, and R. Pastor-Satorras, Phys. Rev. E **78**, 011114 (2008).

[22] Z. Z. Zhang, Y. C. Zhang, S. G. Zhou, M. Yin, and J. H. Guan, J. Math. Phys. **50**, 033514 (2009).

[23] V. Tejedor, O. Bénichou, and R. Voituriez, Phys. Rev. E **80**, 065104(R) (2009).

[24] C. P. Haynes and A. P. Roberts, Phys. Rev. E **78**, 041111 (2008).

[25] J. J. Kozak and V. Balakrishnan, Phys. Rev. E **65**, 021105 (2002).

[26] J. J. Kozak and V. Balakrishnan, Int. J. Bifurcation Chaos Appl. Sci. Eng. **12**, 2379 (2002).

[27] S. Havlin and H. Weissman, J. Phys. A **19**, L1021 (1986).

[28] B. Kahng and S. Redner, J. Phys. A **22**, 887 (1989).

[29] E. Agliari, Phys. Rev. E **77**, 011128 (2008).

[30] R. A. Guyer, Phys. Rev. A **30**, 1112 (1984).

[31] A. Volta, J. Phys. A **42**, 225003 (2009).

[32] A. N. Berker and S. Ostlund, J. Phys. C **12**, 4961 (1979).

[33] Z. Z. Zhang, W. L. Xie, S. G. Zhou, M. Li, and J. H. Guan, Phys. Rev. E **80**, 061111 (2009).

[34] I. Webman and G. S. Grest, Phys. Rev. B **31**, 1689 (1985).

[35] A. Blumen, A. Jurjiu, Th. Koslowski, and Ch. von Ferber, Phys. Rev. E **67**, 061103 (2003).

[36] X. M. Wang, Z. F. Ling, and R. Tao, Phys. Rev. B **45**, 5675 (1992).

[37] C. Stamarel, Ch. von Ferber, and A. Blumen, J. Chem. Phys. **123**, 034907 (2005).

[38] Z. Z. Zhang, S. G. Zhou, L. C. Chen, M. Yin, and J. H. Guan, J. Phys. A **41**, 485102 (2008).

[39] A. Ben-Israel and T. Greville, *Generalized Inverses: Theory and Applications*, 2nd ed. (Springer, New York, 2003).

[40] C. Rao and S. Mitra, *Generalized Inverse of Matrices and Its Applications* (John Wiley and Sons, New York, 1971).

[41] A. García Cantú and E. Abad, Phys. Rev. E **77**, 031121 (2008).

[42] A. K. Chandra, P. Raghavan, W. L. Ruzzo, and R. Smolensky, in *Proceedings of the 21st Annual ACM Symposium on the Theory of Computing* (ACM Press, New York, 1989), pp. 574–586.

[43] P. Tetali, J. Theor. Probab. **4**, 101 (1991).

[44] P. G. Doyle and J. L. Snell, *Random Walks and Electric Networks* (The Mathematical Association of America, Oberlin, OH, 1984); e-print arXiv:math.PR/0001057.

[45] I. Gutman and B. Mohar, J. Chem. Inf. Comput. Sci. **36**, 982 (1996).

[46] H.-Y. Zhu, D. J. Klein, and I. Lukovits, J. Chem. Inf. Comput. Sci. **36**, 420 (1996).

[47] E. Domany, S. Alexander, D. Bensimon, and L. P. Kadanoff, Phys. Rev. B **28**, 3110 (1983).

[48] R. Rammal, J. Phys. (France) **45**, 191 (1984).

[49] C. S. Jayanthi, S. Y. Wu, and J. Cocks, Phys. Rev. Lett. **69**, 1955 (1992).

[50] C. S. Jayanthi and S. Y. Wu, Phys. Rev. B **50**, 897 (1994).

[51] A. Blumen, Ch. von Ferber, A. Jurjiu, and Th. Koslowski, Macromolecules **37**, 638 (2004).

[52] W.-J. Tzeng and F. Y. Wu, Appl. Math. Lett. **13**, 19 (2000).

[53] Z.-G. Huang, X.-J. Xu, Z.-X. Wu, and Y.-H. Wang, Eur. Phys. J. B **51**, 549 (2006).

[54] E. M. Bollt and D. ben-Avraham, New J. Phys. **7**, 26 (2005).

[55] Z. Z. Zhang, Y. Qi, S. G. Zhou, S. Y. Gao, and J. H. Guan, Phys. Rev. E **81**, 016114 (2010).

[56] Z. Z. Zhang, Y. Lin, S. G. Zhou, B. Wu, and J. H. Guan, New J. Phys. **11**, 103043 (2009).

[57] R. Entringer, D. Jackson, and D. Snyder, Czech. Math. J. **26**, 283 (1976).

[58] J. Plesnik, J. Graph Theory **8**, 1 (1984).

[59] W. S. Lovejoy and C. H. Loch, Soc. Networks **25**, 333 (2003).

[60] Z. Z. Zhang, S. G. Zhou, Z. Y. Wang, and Z. Shen, J. Phys. A **40**, 11863 (2007).

[61] A. Ghosh, S. Boyd, and A. Saberi, SIAM Rev. **50**, 37 (2008).

[62] A.-L. Barabási and R. Albert, Science **286**, 509 (1999).

[63] R. Albert and A.-L. Barabási, Rev. Mod. Phys. **74**, 47 (2002).

[64] S. N. Dorogovtsev and J. F. F. Mendes, Adv. Phys. **51**, 1079 (2002).

[65] Z. Z. Zhang, Y. Qi, S. G. Zhou, W. L. Xie, and J. H. Guan, Phys. Rev. E **79**, 021127 (2009).

[66] Z. Z. Zhang, J. H. Guan, W. L. Xie, Y. Qi, and S. G. Zhou, EPL **86**, 10006 (2009).

[67] Z. Z. Zhang, S. G. Zhou, W. L. Xie, L. C. Chen, Y. Lin, and J. H. Guan, Phys. Rev. E **79**, 061113 (2009).

[68] E. Agliari and R. Burioni, Phys. Rev. E **80**, 031125 (2009).

[69] Z. Z. Zhang, Y. Lin, S. Y. Gao, S. G. Zhou, J. H. Guan, and M. Li, Phys. Rev. E **80**, 051120 (2009).